

Inhomogeneous broadening of $\text{Al}_x\text{Ga}_{1-x}\text{N}/\text{GaN}$ quantum wells

F. Natali, D. Byrne, M. Leroux, B. Damilano, F. Semond, A. Le Louarn, S. Veizian, N. Grandjean, and J. Massies
Centre de Recherche sur l'Hétéro-Epitaxie et ses Applications—CNRS, Rue Bernard Grégory, 06560 Valbonne, France
 (Received 17 November 2003; revised manuscript received 10 September 2004; published 15 February 2005)

We report a low-temperature photoluminescence study of a series of $\text{Al}_x\text{Ga}_{1-x}\text{N}/\text{GaN}$ quantum wells of various widths L and with x ranging from 0.11 to 0.25, grown by molecular beam epitaxy on silicon (111) substrates. Such quantum wells are subject to an important Stark effect owing to the large macroscopic polarization (piezoelectric and spontaneous) difference between wells and barriers. Due to the opposite actions of carrier confinement and of the Stark effect on the quantum well transition energies, it appears that around a certain thickness $L_0 \sim 26 \text{ \AA}$, these transition energies are independent of the barrier composition, at least in the x range studied. This has already been reported in similar structures grown on sapphire [Grandjean *et al.*, *J. Appl. Phys.* **86** 3714 (1999)]. In such quantum wells, the inhomogeneous broadening originates essentially from well width fluctuations and alloy composition fluctuations. The effect of the latter is then expected to be minimum near $L=L_0$. We show that it is indeed the case by studying the well width and barrier composition dependence of the linewidth of the quantum well luminescence lines, for samples grown on both Si and sapphire. The x dependence of the minimum linewidth at $L \sim L_0$ allows to estimate a very small variance of the well width distribution ($\sigma_L \sim 1 \text{ \AA}$), and this is discussed in relation with scanning tunneling microscopy images of GaN surfaces. Afterwards, using the fact that confinement energies in wide wells become nearly independent of well width, the variance of barrier composition fluctuations within the excitonic lateral extension is estimated from the L dependence of linewidths at each barrier composition. The values we obtain for this excitonic lateral extension are in agreement with variational calculations of the in-plane exciton Bohr radius in such heterostructures.

DOI: 10.1103/PhysRevB.71.075311

PACS number(s): 78.55.Cr, 78.66.Fd, 78.20.Hp

I. INTRODUCTION

Since in semiconductor quantum wells (QW's) and superlattices the crystal periodicity is not conserved in the growth direction on lengths scales comparable to the de Broglie wavelength of carriers, their electronic states and hence transition energies are strongly influenced by fluctuations in their characteristic lengths.¹ Furthermore, if the well and/or barrier material are based on a solid solution, as for instance in $\text{Al}_x\text{Ga}_{1-x}\text{As}/\text{GaAs}$ quantum wells, (QW's) these states are also influenced by alloy fluctuations within their volume, as they are in bulk semiconductor alloys.² This leads to an inhomogeneous broadening of quantum well exciton energies. At very low temperature, excitons can also localize in shallow potential minima, which also contributes to broadening unless high spatial resolution can be achieved.^{3,4}

Nitride heterostructures grown along the (0001) direction of the wurtzite phase experience a large Stark effect due to interfacial charges induced by the macroscopic polarization discontinuities across their interfaces.⁵ This induces a large redshift of optical transitions with increasing well width, linear for large wells, and a very strong decrease of the optical oscillator strength due to charge separation. Both effects have been clearly seen in the $\text{Al}_x\text{Ga}_{1-x}\text{N}/\text{GaN}$ quantum well case by experiments and confirmed by envelope function calculations of energies and electron-hole overlap integrals.⁶⁻⁹ As a consequence of the opposite actions of carrier confinement that blue-shifts transition energies, and of the Stark effect that red-shifts them, there appears to be a well thickness L_0 near 10 GaN monolayers ($L_0 \sim 26 \text{ \AA}$) where transition energies are nearly independent of the barrier composition,

at least up to $x \sim 0.3$.⁸ Alloy broadening should then be minimum around $L=L_0$. This is what we investigate in the present work through a study of the linewidth of the low-temperature luminescence of $\text{Al}_x\text{Ga}_{1-x}\text{N}/\text{GaN}$ quantum wells grown on (111) silicon with various widths and barrier compositions.

II. EXPERIMENTAL DETAILS AND RESULTS

The investigated samples are grown on (111) silicon by molecular beam epitaxy using NH_3 as nitrogen precursor. An $\text{AlN}/\text{GaN}/\text{AlN}$ buffer sequence is first grown on Si,¹⁰ then a relaxed (more than $1 \mu\text{m}$ thick) $\text{Al}_x\text{Ga}_{1-x}\text{N}$ layer is grown. On these templates, samples containing up to six GaN single QW's with thicknesses L ranging from 4 to 30 molecular monolayers (ML's, $1 \text{ ML} = 2.59 \text{ \AA}$) were grown. The QW's are grouped by two, separated by a 100-\AA barrier, and each pair of QW's is separated from the others by 500-\AA -wide barriers. A 600-\AA -thick $\text{Al}_x\text{Ga}_{1-x}\text{N}$ cap layer is finally grown. Photoluminescence (PL) was performed at 11 K in a closed-cycle He cryostat. A 64-cm focal length monochromator equipped with a 1200-grooves/mm grating was used, with a slit width-limited resolution of 1.2 \AA . A frequency-doubled Ar laser was used for excitation ($\lambda = 244 \text{ nm}$). The maximum incident power is $\sim 15 \text{ W/cm}^2$; under these conditions the screening of the Stark field by photoexcited carriers is negligible.⁸ Images of GaN (0001) surfaces were obtained with a scanning tunneling microscope (STM) coupled under ultra high vacuum ($P \approx 5 \times 10^{-11}$ Torr) to a nitride-dedicated molecular beam epitaxy machine.

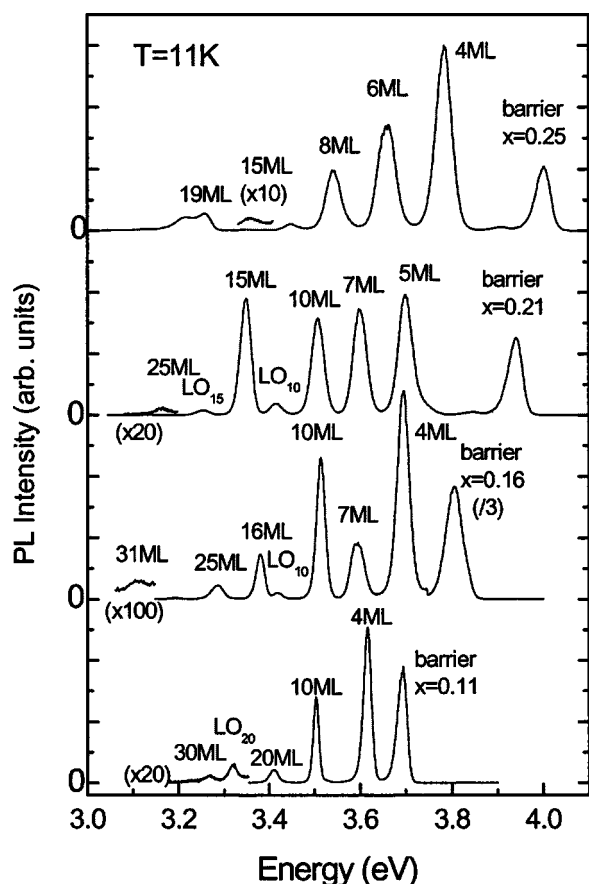


FIG. 1. Photoluminescence spectra at 11 K of $\text{Al}_x\text{Ga}_{1-x}\text{N}/\text{GaN}$ quantum well samples grown on silicon with various barrier compositions. Each QW lines are labeled according to their width in GaN monolayers (ML's). The spectra are shifted vertically for clarity.

Figure 1 displays the PL spectra of four QW samples with barrier compositions increasing from 0.11 to 0.25. Near-edge PL from the barriers is observed, together with the QW luminescence bands, labelled according to their width in monolayers (lines labeled LO_n are LO-phonon replicas of line n). As for similar QW's grown by molecular beam epitaxy on sapphire,⁸ one observes a fanlike variation of PL energies with increasing barrier composition: narrow wells, very sensitive to confinement, increase in energy with x ; large wells, mostly sensitive to the Stark field, decrease in energy with x . One also notes that the luminescence from wide wells is very weak. This is not only due to their larger distance from the sample surface, but also to their long radiative lifetimes, owing to a large electron-hole spatial separation.^{6-9,11}

The well width dependence of PL energies for each barrier composition is given in Fig. 2. In the framework of macroscopic polarization, the excitonic ground-state transition energies in such quantum wells is given by

$$\begin{aligned}
 E(x,L) &= E_G(\text{GaN}) + E_1(x,L) + H_1(x,L) - \mathcal{R}(x,L) - qF(x)L \\
 &= E_G(\text{GaN}) + E_c(x,L) - qF(x)L,
 \end{aligned}
 \tag{1}$$

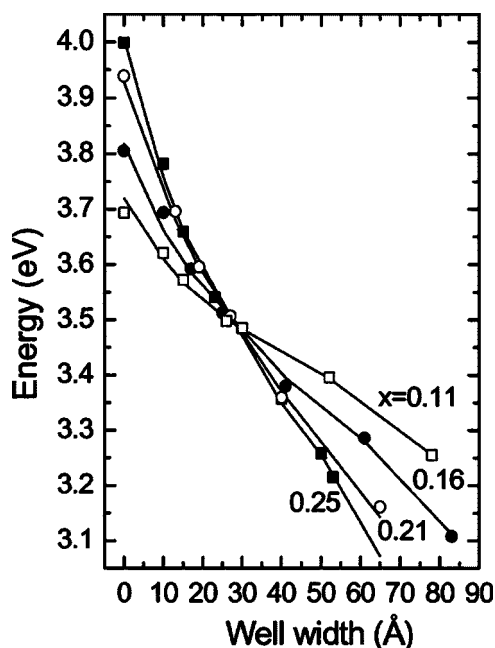


FIG. 2. Quantum well luminescence energies as a function of well width (symbols). The solid lines are the calculated energies.

where $E_G(\text{GaN})$ is the GaN band gap, E_1 and H_1 are the ground-state electron and hole confinement energies, \mathcal{R} is the excitonic Rydberg constant, q the elementary charge, and F the built-in electric field. Confinement energies and Rydberg constants were calculated within the envelope function formalism using a transfer matrix method, using the electric field F as a parameter. Details of these calculations and the material parameters used are given in Ref. 8. The results are shown as solid lines in Fig. 2, showing that a good agreement with experiment is obtained. The calculated $E(L,x)$ curves show some irregularities, for two reasons. The first is that at low temperature, luminescence involves excitons localized on local potential minima. The calculations are corrected for the localization energies, which we determine experimentally from the S-shape dependence of the QW energies versus temperature.⁷ The other reason is that in our samples, barriers have a finite width. The electric field induced by the polarization discontinuities at interfaces redistributes between wells and barriers.^{7,8,12} As such, the field in the wells is reduced from its value expected for infinite barriers by a geometrical factor. In the present case, this geometrical factor varies from 0.85 for wide wells to 0.95 for narrow ones.

In Fig. 3 the x dependence of the electric field is plotted, deduced for the case of infinite barriers [for (0001)-grown heterostructures, $|F| = |\Delta P| / \epsilon \epsilon_0$, where ΔP is the polarization discontinuity, ϵ the static dielectric constant, and ϵ_0 the permittivity of vacuum]. We also plot similar results for $\text{Al}_x\text{Ga}_{1-x}\text{N}/\text{GaN}$ QW's grown on sapphire by molecular beam epitaxy in our laboratory.^{7,8} Both sets of data are in good agreement. The electric field increases linearly with x in the investigated range and $F \sim 6x$ MV/cm. Our QW's are strained to the $\text{Al}_x\text{Ga}_{1-x}\text{N}$ barriers, whereas in the samples of references,^{7,8} barriers were strained to GaN. We could expect slightly smaller field values in our case compared to the case

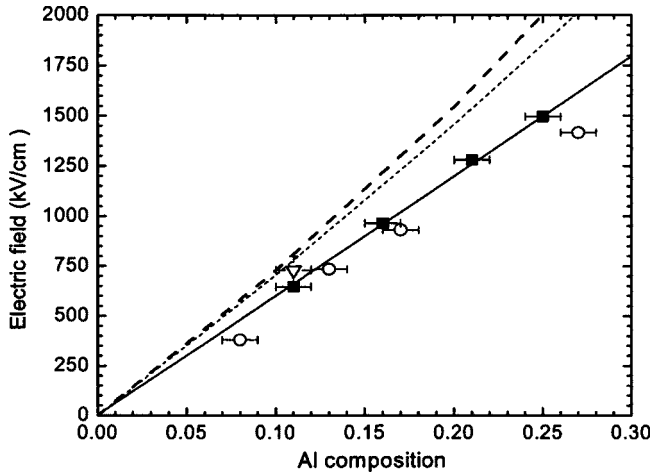


FIG. 3. Electric field in single GaN quantum wells as a function of barrier composition deduced from the data of Fig. 2 (solid squares). Open triangles and circles are field values for similar samples grown on sapphire, from Refs. 7 and 8, respectively. The dashed and dotted lines are the theoretical field values for samples strained to GaN or to the barriers, respectively.

of in Refs. 7 and 8, since the piezoelectric constants of GaN are smaller than those of AlN, and hence of $\text{Al}_x\text{Ga}_{1-x}\text{N}$.^{5,13} We also plot in Fig. 3 the theoretically expected field values for structures strained to GaN or to the barriers, taking into account recent calculations on the nonlinear dependence of polarizations in nitride alloys.¹³ Our values are slightly smaller than the theoretical ones, as already reported.^{7,8}

A salient feature in Fig. 2 is that a singular point in the $E(x, L)$ curves exists: for $L=L_0 \sim 10$ ML (26 Å), the QW energies are nearly independent of the barrier composition. This was already reported in Ref. 8 for QW's grown on sapphire, at precisely the same width, and is well reproduced by our calculations. It is then to be expected that random alloy broadening should be minimum near $L=L_0$. This is exactly what is observed in Fig. 4, displaying the full width at half maximum (linewidth Δ) of the quantum well PL lines as a function of L . We also report in Fig. 4 data from the spectra in Ref. 8, where again a minimum in Δ is observed around L_0 . This is thus a reproducible effect, whose implications are discussed in the next part. Note that a similar study of the PL broadening of $\text{Al}_{0.15}\text{Ga}_{0.85}\text{N}/\text{GaN}$ QW's grown by metalorganic vapor phase epitaxy was already published four years ago.¹⁴ The linewidths observed at that time were larger than those reported in our work, and increase monotonically with well width. This shows that stronger fluctuations, or other broadening mechanisms, are present in the QW samples of Ref. 14 relative to ours.

III. DISCUSSION

In this section, we shall try to put forward the leading terms acting on the inhomogeneous broadening of the QW energies. Following Eq. (1) we may write for the effect of well width or random alloy fluctuations:

$$dE(x, L) = (\partial E_c / \partial L - q\alpha x)dL + (\partial E_c / \partial x - q\alpha L)dx, \quad (2)$$

where we have used the linear dependence of electric field with x (Fig. 3), $F = \alpha X$, with $\alpha \sim 0.9 \times 6 = 5.4$ MV/cm. The

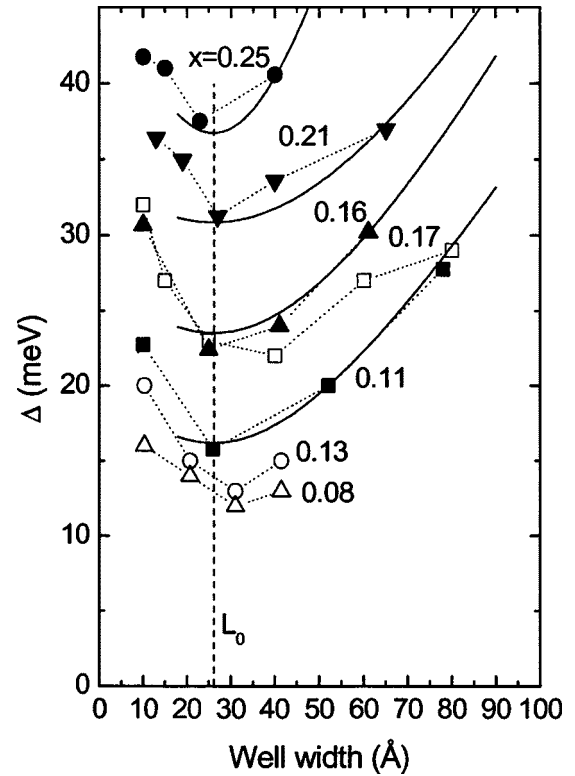


FIG. 4. Well width dependence of quantum well luminescence linewidths for various barrier compositions. Solid symbols come from the present work, open symbols from Ref. 8. The solid curves are calculated according to Eq. (5).

factor 0.9 is an average of the geometrical factor previously mentioned. From Fig. 2 we know that

$$(\partial E_c / \partial x)_{L=L_0} \sim q\alpha L_0 \quad \forall x. \quad (3)$$

Then $E_c(x, L_0) = q\alpha x L_0 - \mathcal{R}(\text{GaN})$ since $E_1(0, L) = H_1(0, L) = 0$. This shows that the energy corresponding to the singular point is the excitonic band gap of GaN, as experimentally shown in Fig. 2 and in Ref. 8.

We plot in Fig. 5 the x dependence of the minimum linewidths, around $L=L_0$, reported in Fig. 4. It increases linearly with x , as could be expected from Eq. (2). Indeed, as Fig. 2 shows, QW's of width L_0 are almost in the linear Stark effect regime, valid for wide wells.¹ In this regime, confined states lie deep in the triangular wells and confinement energies become independent of well width, since each carrier is pushed far apart from one barrier. It is sometimes assumed that since in $\text{Al}_x\text{Ga}_{1-x}\text{N}/\text{GaN}$ heterostructures the effective masses and band offsets are large, their electronic states are close to the infinitely deep well case. The sum of the electron and hole ground-state confinement energies in an infinite triangular well is¹

$$E_1 + H_1 = 1.84[(h^2/m_e)^{1/3} + (h^2/m_h)^{1/3}](qF)^{2/3}, \quad (4)$$

where m_e and m_h are the electron and hole masses. However, Eq. (4) strongly overestimates confinement energies, as shown by comparing with our envelope function calculations. Figure 6 shows the well width dependence of E_c for x

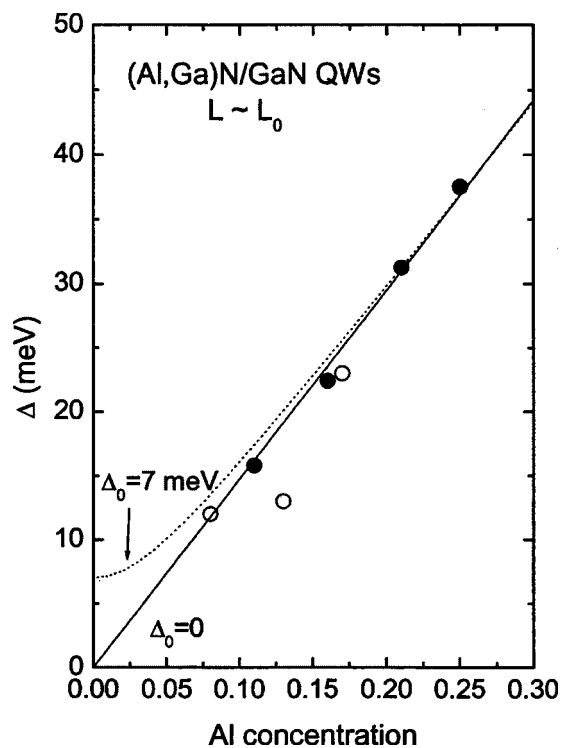


FIG. 5. Barrier composition dependence of the minimum luminescence linewidth at well thicknesses near L_0 . Solid symbols, present work; open symbols, Ref. 8.

in the 0–0.3 range. For $L > L_0$, these energies become indeed almost independent of well width. Actually, Fig. 6 shows that E_c slightly increases with L for wide wells. This is due to the fact that confinement energies E_1 and H_1 become constant, but the excitonic Rydberg constant still decreases slowly with increasing L .^{8,11} We find that the asymptotic values of E_1 and H_1 vary rather as $x^{0.75}$ than as $x^{2/3}$. We can also see from Fig. 6 that for $L=L_0$, the slope of the Stark term $-q\alpha xL$ is much larger than that of confinement energies, i.e., we can neglect $\partial E_c/\partial L$ in front of $-q\alpha x$ in the first term of Eq. (2), when $L \geq L_0$.

For independent variables, variances add quadratically and for a Gaussian distribution, the variance σ and the linewidth Δ are proportional [$\Delta=2(2 \ln 2)^{1/2}\sigma$], we then write in the general case, when $L \geq L_0$:

$$\Delta_E^2 \sim \Delta_0^2 + q^2 \alpha^2 x^2 \Delta_L^2 + (\partial E_c/\partial x - q\alpha L)^2 \Delta_x^2, \quad (5)$$

where we have included an inhomogeneous broadening of the GaN excitonic gap Δ_0 . In thick GaN samples grown by molecular beam epitaxy on Si, excitonic linewidths are in the 6–8 meV range, owing mainly to strain inhomogeneities.¹⁰ For a GaN QW, the strain inhomogeneity along the growth direction is negligible, but not the lateral one (it is principally due to threading dislocations). We plot in Fig. 5 the quantity $(\Delta_0^2 + q^2 \alpha^2 x^2 \Delta_L^2)^{1/2}$ with Δ_L as a parameter, for both $\Delta_0=0$ or 7 meV. In both cases, we find $\Delta_L=2.7 \text{ \AA}$, i.e., about 1 ML. The variance of the well width distribution is $\sigma_L=1.1 \text{ \AA}$. For uncorrelated interfaces, the interface width should have a variance of $\sim 1.1/\sqrt{2}=0.8 \text{ \AA}$.

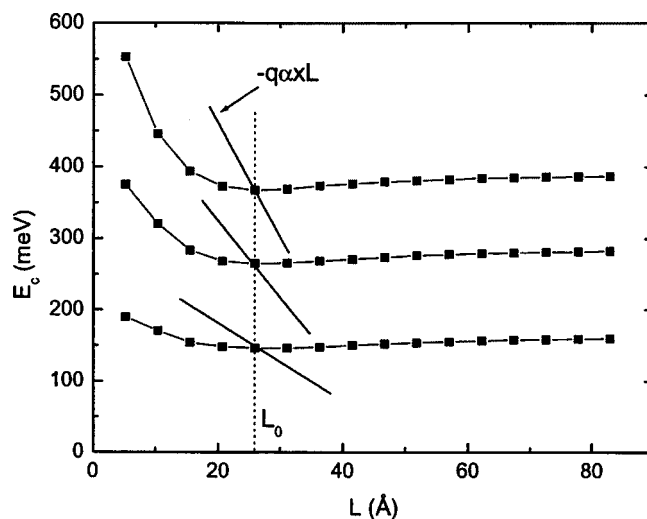


FIG. 6. Calculated well width dependence of E_c , sum of the electron and hole confinement energies minus the exciton Rydberg constant in $\text{Al}_x\text{Ga}_{1-x}\text{N}/\text{GaN}$ quantum wells, with x in the 0–0.3 range. The Stark term $-q\alpha xL$ is also shown.

This distribution may look narrow. To see if this is realistic, a STM study of GaN (0001) surfaces have been performed. The samples are grown on (111) Si, as our QW's. STM images are given in Fig. 7. The GaN surface is $(2 \times 2)\text{-N}$ reconstructed, which is typical of Ga polarity surfaces obtained in molecular beam epitaxy growth using NH_3 as nitrogen source.¹⁵ This surface is composed of very flat terraces, separated by one monolayer high steps. Since most of these terraces are larger than the exciton Bohr radii,¹¹ and knowing that steps at quantum well interfaces are repulsive for excitons,¹⁶ it is reasonable to assume that PL originates mainly from such type of terraces. The root-mean-square roughness (i.e., the height variance) on a terrace, for surfaces of a few tens of nanometers in size varies from 0.3 to 0.8 \AA . But in such a well-defined crystallographic plane, such a “roughness” comes from slight variations of electronic density of states and not from a “true” topographic roughness, though it can include a topographic contribution (vacancies, adatoms, etc.). As such the agreement with our PL determination of the interface roughness has no true physical significance, but it means that QW interfaces are very flat at the scale of excitons. As such, these STM images are in qualitative agreement with the small well width variance we deduced from PL linewidths.

We mentioned previously that at low temperature ($T=11 \text{ K}$), the QW excitons we observe are localized. This can be checked by the S-shape dependence of the PL energy versus temperature, clearly evidencing exciton delocalization, or by comparison between low-temperature PL and reflectivity features.⁷ The low-temperature PL involves regions that are typically 1–2 ML thicker than the average.^{7,8} The vision we obtain then is that of excitons on regions slightly thicker than the average, but composed of large terraces, with no evidence for microroughness as is the case for (2×4) reconstructed GaAs (001) surfaces.⁴ This would be in agreement with the STM images and also the fact that the exciton lateral extension that we estimate in the following is

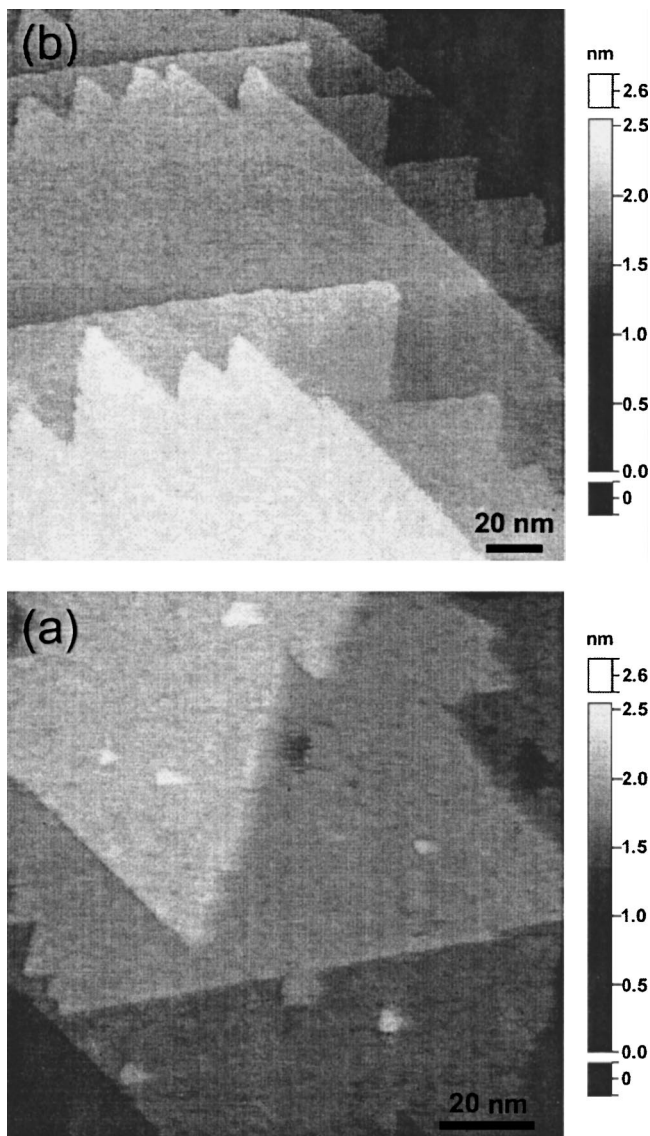


FIG. 7. Scanning tunneling microscopy images of the GaN (0001) (2×2) -N surface at different locations. (a) $100 \times 100 \text{ nm}^2$; empty states (+2 V, 0.01 nA); (b) $200 \times 200 \text{ nm}^2$; empty states (+4 V, 0.3 nA).

in the range of free-exciton in-plane Bohr radii.

We shall now use the well width dependence of Δ_E for $L \geq L_0$ (Fig. 4), to estimate the importance of alloy disorder. First, we assume that Δ_L is independent of L . Second, we need to know $\partial E_c / \partial x$ [see Eq. (5)]. As mentioned above, no simple approximation holds for $E_c(x, L)$. But we know from the previous discussion that $(\partial E_c / \partial x)_{L=L_0} = q\alpha L_0$ [Eq. (3)]. Since there are no accidents in the $E_c(x, L)$ variations, we shall consider this value as a valid approximation for $L > L_0$. We can then calculate the well width dependence of the PL linewidths for any x and $L \geq L_0$, using the width of the random alloy distribution Δ_x as a fitting parameter. This is shown as solid curves in Fig. 4 for each barrier composition studied. For QW's with barrier compositions of 0.11, 0.16, 0.21, and 0.25, we obtain $\Delta_x = 8.4 \times 10^{-3}$, 1×10^{-2} , 1×10^{-2} , and 2.2×10^{-2} respectively, the last value having a very large

uncertainty since it relies on one point only. To make the link with other physical parameters, we use

$$\Delta_x = 2(2 \ln 2)^{1/2} \sigma_x = 2(2 \ln 2)^{1/2} [x(1-x)/d_{\text{III}}S]^{1/2}, \quad (6)$$

where d_{III} is the areal density of cations sites in a (0001) plane ($d_{\text{III}} = 1.36 \times 10^{15} \text{ cm}^{-2}$) and S is the lateral extension of QW excitons. Equation (6) is the direct equivalent in the two-dimensional case of the three-dimensional case studied in Ref. 2. Using $S = \pi \langle r^2 \rangle$, and $\langle r^2 \rangle = 3\rho^2$, where ρ is an in-plane excitonic Bohr radius, we obtain $\rho = 77, 76, 85$, and 40 \AA for $x = 0.11, 0.16, 0.21$, and 0.25 respectively. Actually, alloy fluctuations are not expected to be correlated between the two barriers. Since one plane of interfacial polarization charges induces a field $F/2$, and since variances add quadratically, the above results should be divided by $\sqrt{2}$, leading to $\rho \sim 50 \text{ \AA}$. It is now interesting to compare such value with what we know of the in-plane extension of excitons in $\text{Al}_x\text{Ga}_{1-x}\text{N}/\text{GaN}$ QW's. Bigenwald *et al.*,¹¹ using a three-dimensional variational wave function, have calculated the Rydberg and Bohr radii of such excitons. As a function of well width, the in-plane Bohr radius first decreases from its GaN value, due to the confinement-induced strengthening of the Coulomb attraction, and then increases due to the Stark-effect-induced loosening of this attraction. For a barrier composition $x = 0.27$, and for well widths varying from 26 to 80 \AA (the range from which we deduced σ_x , i.e., ρ), the in-plane Bohr radius increases from 35 to 75 \AA . The lateral extension of excitons we estimate from our study of PL linewidth is then well within the range of the calculated in-plane Bohr radii of similar quantum well excitons.

The Gaussian distribution is the large number limit of the binomial distribution. Considering the multiplying factor in front of Δ_x in Eq. (5), we see that for wide wells ($L \geq L_0$), it involves almost only the Stark field, firstly via $\partial E_c / \partial x$, only related to α in our approximation, and secondly via $q\alpha L$, describing the band-gap drop due to F . These are the two reasons why random alloy fluctuations are so important in our structures, though the well material is a true binary compound. This is a great difference with the $\text{Al}_x\text{Ga}_{1-x}\text{As}/\text{GaAs}$ QW case, where alloy fluctuations act through band offset fluctuations and exciton wave function penetration in the barriers. As such, their effect are weak in wide $\text{Al}_x\text{Ga}_{1-x}\text{As}/\text{GaAs}$ wells. In contrast, in $\text{Al}_x\text{Ga}_{1-x}\text{N}/\text{GaN}$ QW's, since the Coulomb interaction is long range, the effect of alloy fluctuations is strong along the whole QW thickness. From the macroscopic polarization point of view, the Stark effect originates from two planar interfacial charges. If we now consider the quantum well volume as composed of [0001] atomic columns, the use of a binomial distribution means that if the exciton in its trajectory faces a Ga atom at the interface, the effect is null on the energy, while if it faces an Al atom, the total AlN/GaN polarization discontinuity is experienced. The result is an average, virtual-crystal-like polarization difference. In that sense, if our interpretation of PL broadening is correct, it can be said that our results make a link from the experimental side between microscopic dipole differences and macroscopic polarization, as it is done from the theoretical side.^{5,13}

Before concluding, a few remarks are necessary on the validity of the parameters used in the envelope function calculations. It is a two-band model. Some parameters are poorly known experimentally in nitrides, in particular band offsets and hole masses, and hence their alloy dependence. The model considers only one hole band, though the ground-state valence band symmetry changes with x in $\text{Al}_x\text{Ga}_{1-x}\text{N}$,¹⁷ and this acts too on the QW hole symmetry.¹⁸ Actually, considering the work performed here, the only important point is that these calculations reproduce fairly well the experimental results, in particular the singular point around L_0 (Fig. 2), and give reasonable field values, increasing linearly with x in the investigated range (Fig. 3).

IV. CONCLUSIONS

We have studied the well width and composition dependence of the luminescence linewidth of $\text{Al}_x\text{Ga}_{1-x}\text{N}/\text{GaN}$ QW's. This linewidth is minimum near a QW width of 26 Å, where energies are nearly independent of barrier compositions. From our data, we deduce a small variance of the well width distribution, in qualitative agreement with a STM

study of GaN surfaces, and an estimate of the exciton in-plane extension in wide wells. The Stark effect plays a crucial role in enhancing the importance of alloy fluctuations. Though they are minimum around $L=26$ Å, owing to the long-range nature of the Coulomb interaction they still have a great importance in the luminescence broadening for wide wells, contrary to the $\text{Al}_x\text{Ga}_{1-x}\text{As}/\text{GaAs}$ QW case.

In cases where inhomogeneous broadening is an important issue, such as for instance $\text{Al}_x\text{Ga}_{1-x}\text{N}/\text{GaN}$ QW-based microcavity structures working in the strong light-matter coupling regime, thicknesses near 26 Å could be optimum, since in such narrow enough wells the reduction of the optical oscillator strength by the Stark effect is only a factor of 4 relative to the bulk value. However, for polariton-based device structures the exciton binding energy will be decisive for room-temperature operation. It may thus be more advantageous for these structures to use a 15-Å quantum well whose exciton binding energy and oscillator strength remain relatively large due to confinement while its inhomogeneous broadening is just slightly broader than the minimum value at L_0 .

¹G. Bastard, *Wave Mechanics Applied to Semiconductor Heterostructures* (Les Editions de Physique, Les Ulis, 1996).

²E. F. Schubert, E. O. Göbel, Y. Horikoshi, K. Ploog, and H. J. Queisser, *Phys. Rev. B* **30**, 813 (1984).

³C. D. Warwick and R. F. Kopf, *Appl. Phys. Lett.* **60**, 386 (1992).

⁴R. Grousson, V. Voliotis, N. Grandjean, J. Massies, M. Leroux, and C. Deparis, *Phys. Rev. B* **55**, 5253 (1997).

⁵F. Bernardini, V. Fiorentini, and D. Vanderbilt, *Phys. Rev. B* **56**, R10 024 (1997).

⁶J. S. Im, H. Kollmer, J. Off, A. Sohmer, F. Scholz, and A. Hangleiter, *Phys. Rev. B* **57**, R9435 (1998).

⁷M. Leroux, N. Grandjean, M. Läügt, J. Massies, B. Gil, and P. Lefebvre, *Phys. Rev. B* **58**, R13 371 (1998).

⁸N. Grandjean, B. Damilano, S. Dalmaso, M. Leroux, M. Läügt, and J. Massies, *J. Appl. Phys.* **86**, 3714 (1999).

⁹P. Lefebvre, J. Allègre, B. Gil, H. Mathieu, N. Grandjean, M. Leroux, J. Massies, and P. Bigenwald, *Phys. Rev. B* **59**, 15 363 (1999).

¹⁰F. Semond, Y. Cordier, N. Grandjean, F. Natali, B. Damilano, S. Vézian, and J. Massies, *Phys. Status Solidi A* **188**, 501 (2001).

¹¹P. Bigenwald, P. Lefebvre, T. Bretagnon, and B. Gil, *Phys. Status Solidi B* **216**, 71 (1999).

¹²M. Leroux, N. Grandjean, J. Massies, B. Gil, P. Lefebvre, and P. Bigenwald, *Phys. Rev. B* **60**, 1496 (1999).

¹³F. Bernardini and V. Fiorentini, *Phys. Rev. B* **64**, 085207 (2001).

¹⁴A. Hangleiter, J. S. Im, J. Off, and F. Scholz, *Phys. Status Solidi B* **216**, 427 (1999).

¹⁵S. Vézian, F. Semond, J. Massies, D. W. Bullock, Z. Ding, and P. M. Thibado, *Surf. Sci.* **541**, 242 (2003).

¹⁶B. Chastaingt, M. Leroux, G. Neu, N. Grandjean, C. Deparis, and J. Massies, *Phys. Rev. B* **47**, 1292 (1993).

¹⁷M. Leroux, S. Dalmaso, F. Natali, S. Hélin, C. Touzi, S. Läügt, M. Passerel, F. Omnes, F. Semond, J. Massies, and P. Gibart, *Phys. Status Solidi B* **234**, 887 (2002).

¹⁸P. A. Shields, R. J. Nicholas, N. Grandjean, and J. Massies, *Phys. Rev. B* **63**, 245319 (2001).